

Enhanced apoptosis in retinal pigment epithelium under inflammatory stimuli and oxidative stress

Yujuan Wang · Defen Shen · Vinson M. Wang ·
Cheng-Rong Yu · Ren-Xi Wang · Jingsheng Tuo ·
Chi-Chao Chan

Published online: 22 August 2012
© Springer Science+Business Media, LLC (outside the USA) 2012

Abstract Age-related macular degeneration (AMD) is a neurodegenerative disease that causes irreversible central vision loss in the elderly. Retinal pigment epithelium (RPE) has been found to be a key component in AMD pathogenesis. The *Ccl2*^{-/-}/*Cx3cr1*^{-/-} (DKO) mouse on *Crb1*^{rd8} background is created as an AMD model, developing AMD-like retinal lesions. Our study aimed to examine RPE apoptosis in DKO mouse and human ARPE-19 cell line. DKO RPE expressed higher apoptotic proteins when compared with age-matched wild type (WT) RPE in physiological conditions. Apoptosis of primary cultured mouse RPE was evaluated under stimulation with lipopolysaccharide for inflammatory stimulation and 2,3,7,8-tetrachlorodibenzo-*p*-dioxin or H₂O₂ for oxidative stress. Compared with WT RPE, DKO RPE was more susceptible to Fas ligand (FasL)-mediated apoptosis under both inflammatory and oxidative stress, with less cell viability and higher expression of apoptotic transcripts and proteins. Decreased cell viability was also observed in ARPE-19 cells under each stimulus. Furthermore, we also investigated the anti-apoptotic effects of decoy receptor 3 (DcR3), a decoy receptor for FasL, on ARPE-19 cells under inflammatory and oxidative stress. DcR3 pre-incubated ARPE-19 cells

showed decreased apoptosis, with increased cell viability and decreased expression of apoptotic transcripts and proteins under the stimuli. On the contrary, knockdown of DcR3 in ARPE-19 cells showed totally opposite results. Our study demonstrates that FasL-mediated RPE apoptosis may play a pivotal role in AMD pathogenesis.

Keywords Apoptosis · Retinal pigment epithelium (RPE) · Inflammation · Oxidative stress · Fas ligand (FasL) · Decoy receptor 3 (DcR3)

Introduction

Age-related macular degeneration (AMD) is a chronic, degenerative disorder in the maculae of the retina. It has become the leading cause of irreversible central vision impairment among the elderly [1–4]. Clinically, two subtypes of AMD are geographic atrophy (dry) AMD and neovascular, exudative (wet) AMD [3]. Geographic atrophy AMD accounts for the majority of all diagnosed AMD cases and is characterized by the presence of drusen, degeneration of retinal pigment epithelium (RPE) and photoreceptors in the maculae [5]. The hallmark of neovascular AMD is the presence of choroidal neovascularization (CNV) in the maculae, leading to exudation and fibrovascular scarring in the end stage. Although the pathogenesis of AMD is complex and not fully understood, RPE is one of the central cells in the initiation and progression of AMD [6, 7].

The RPE is a monolayer of hexagonal, cuboidal cells located between the photoreceptors and Bruch's membrane-choroid complex. It has a very high metabolic rate and is indispensable for the visual process conducted by

Y. Wang · D. Shen · V. M. Wang · J. Tuo · C.-C. Chan (✉)
Immunopathology Section, Laboratory of Immunology, National Eye Institute, National Institutes of Health, 10 Center Dr., 10/10N103, NIH/NEI, Bethesda, MD 20892-1857, USA
e-mail: chanc@nei.nih.gov

Y. Wang
Zhongshan Ophthalmic Center, Sun Yat-sen University,
Guangzhou 510060, China

C.-R. Yu · R.-X. Wang
Molecular Immunology Section, Laboratory of Immunology,
National Eye Institute, National Institutes of Health, Bethesda,
MD 20892, USA

photoreceptors and other retinal neurons [8]. Physiologically, the function of the RPE includes phagocytosis of the shed outer segments of photoreceptors, and transportation of nutrients to the choroid and retina. It also absorbs light and forms the outer blood-ocular barrier in the retina. Additionally, the RPE has regulatory actions in innate and adaptive immune responses and produces a variety of cytokines, mainly pro-inflammatory ones [8–10]. RPE is critical for the maintenance and survival of the photoreceptors and plays an important role in AMD pathogenesis [6, 8].

Both local inflammation and oxidative stress are related with RPE apoptosis in AMD [11–14]. An accumulation of insoluble, extracellular deposits (drusen) beneath the RPE in Bruch's membrane elicits local chronic inflammation, complement activation, and immune responsiveness [15]. These inflammatory responses may compromise RPE function and exacerbate the pathogenesis of AMD [12, 15]. Besides inflammation, oxidative stress through the release of reactive oxygen species is a crucial trigger for AMD pathogenesis. RPE is susceptible to oxidative stress in several aspects. Phagocytosis of high concentrations of polyunsaturated fatty acids from photoreceptor outer segments, and high oxygen tension in the maculae generated by the RPE induces extensive oxidative stress [16, 17]. Additionally, the antioxidant capacity of the RPE decreases with age, which further provides an oxidative burden to the retina [18, 19]. Several studies have shown that oxidative stress in RPE plays a pivotal role in AMD pathogenesis [20–22].

Apoptosis is regulated by a series of signal cascades under certain situations. There are two principal apoptotic pathways, an extrinsic or death receptor pathway triggered by Fas ligand (FasL) and Fas interaction on the cellular membrane, and an intrinsic or mitochondrial pathway triggered through the *Bcl-2* gene family, leading to release of cytochrome c and activation of caspase-9. These two pathways are linked together and the molecules in one pathway can influence the other [23]. Decoy receptor 3 (DcR3), a soluble receptor, is a new member of the tumor necrosis factor (TNF) receptor superfamily. An important function of DcR3 is to act as a decoy receptor that competitively binds with FasL [24, 25]. Because DcR3 lacks a transmembrane domain, it does not transduce apoptotic signals. But rather, it neutralizes the biological effects of FasL by interfering with FasL-mediated apoptosis. DcR3 is overexpressed in tumor cells, including lung cancers and gastrointestinal tract tumors [24, 26]. In addition, DcR3 is also expressed in some normal tissues, such as the fetal lung, brain, and liver, and in the adult spleen, colon, and lung [24, 26]. However, the expression and anti-apoptotic effects of DcR3 have not been investigated in RPE cells.

In this study, we examine the differences in regulation of apoptosis between primary cultured RPE of *C57/B6* wild type (WT) and *Ccl2^{-/-}/Cx3cr1^{-/-}* mouse on retinal degeneration (rd) 8 background, *Crb1^{rd8}* (DKO, an AMD murine model),

under inflammatory stimuli and oxidative stress. Additionally, we evaluate the anti-apoptotic effects of DcR3 in a human RPE cell line ARPE-19 under such stress.

Materials and methods

Animals

The development of DKO mice on *Crb1^{rd8}* background was described previously [27, 28]. The DKO mice and age-matched WT mice were bred in-house. All animal experiments were performed under protocols approved by the National Eye Institute Institutional Animal Care and Use Committee and were in compliance with the ARVO Statement for the Use of Animals in Ophthalmic and Vision Research.

Cell culture

ARPE-19 cells were obtained from the American Type Culture Collection (Manassas, VA, USA) and cultured in DMEM/F12 medium (1:1) (Sigma-Aldrich, St Louis, MO, USA) containing 10 % fetal bovine serum (FBS, Sigma-Aldrich) and 1 % L-glutamine–penicillin–streptomycin (Sigma-Aldrich). The cells were cultured at 5 % CO₂/37 °C condition and split when approximately 90 % confluent. RPE cells between six and eight passages were taken for the experiments.

Isolation and culture of primary mouse RPE cells

Mouse RPE was isolated from retinas of WT and DKO mice of 4–8 weeks old. Briefly, experimental animals were euthanized and their eyes were enucleated. The globes were dissected free of periocular connective tissue, transferred into 2 % Dispase II (neutral protease, grade II, Roche, Indianapolis, IN, USA) in phosphate-buffered saline (PBS), and incubated at 37 °C for 40–45 min. Dispase II activity was terminated by washing the globes three times in DMEM/F12 medium plus 15 % FBS. The anterior segment was removed and the retina was dissected free from the underlying RPE-choroidal eyecups. The loosely adherent RPE cell layer was gently separated from the choroid and transferred to a 15 ml tube containing DMEM/F12, 15 % FBS, and 1 % L-glutamine–penicillin–streptomycin. The RPE suspension was planted on 6-well cell culture plates at 5 % CO₂/37 °C. The medium was changed after 5–6 days, and every 2–3 days thereafter. The RPE cells grew to form a confluent cell layer by 2–3 weeks and were used for experiments between two and three passages.

LPS, TCDD, and H₂O₂ stimulation of RPE cells

Primary mouse RPE and ARPE-19 cells grown to 90 % confluence in culture plates were incubated in serum-free

culture medium for 24 h, and subsequently with various concentrations of lipopolysaccharide (LPS, Sigma-Aldrich), 2,3,7,8-tetrachlorodibenzo-*p*-dioxin (TCDD, Sigma-Aldrich), or H₂O₂ (Sigma-Aldrich). Inflammatory stress was induced by LPS: mouse RPE cells were stimulated with 1 µg/ml LPS while ARPE-19 cells were stressed with 10, 50, and 100 µg/ml LPS in serum-free culture medium for 24 h. Oxidative stress was induced by TCDD or H₂O₂ as follows: mouse RPE cells were stimulated with 1 nM TCDD (dissolved in less than 0.05 % dimethyl sulfoxide (DMSO, Sigma-Aldrich)) while ARPE-19 cells with 10, 50, and 100 nM TCDD in serum-free culture medium for 24 h; mouse RPE cells were stimulated with 100 µM H₂O₂ while ARPE-19 cells with 100, 200 µM and 1 mM H₂O₂ in serum-free culture medium for 2 h.

Preincubation of ARPE-19 cells with DcR3-Fc protein

ARPE-19 cells were pretreated with 0.3 µg/ml recombinant human DcR3-Fc chimera protein (DcR3-Fc, R&D Systems, Minneapolis, MN, USA) or control rhIgG1-Fc (R&D Systems) for 24 h in serum-free DMEM/F12 medium. The cells were washed twice with PBS before LPS, TCDD, or H₂O₂ stimulation.

Transfection of DcR3 siRNA into ARPE-19 cells

DcR3 small interfering RNA (DcR3 siRNA, Santa Cruz Biotechnology, Santa Cruz, CA, USA) and nonspecific control siRNA (Santa Cruz) were transfected into ARPE-19 cells using transfection reagent according to the protocol of the manufacturer. Briefly, for each transfection, 4 µl siRNA and 6 µl siRNA transfection reagent (Santa Cruz) were diluted into 1 ml siRNA transfection medium (Santa Cruz). The cells were washed once with 2 ml transfection medium. The diluted mixture was applied to 1×10^6 ARPE-19 cells and incubated for 6 h. The mixture was replaced with DMEM/F12 plus 10 % FBS and incubated for 6, 12, or 24 h before RNA extraction and immunohistochemistry.

Measurement of mitochondrial damage by MTT assay

The assessment of mitochondrial damage was performed using a 3-(4,5-dimethylthiazol-2-yl)-2,5-diphenyl tetrazolium bromide (MTT) assay in primary mouse RPE and ARPE-19 cells. Briefly, the cells were seeded at 1×10^5 cells per well in 96-well culture plates and the adherent cells were starved with serum-free culture medium. After LPS, TCDD, or H₂O₂ stimulation for the indicated time periods, the cells were washed with PBS and incubated with 20 µl of stock MTT solution (5 mg/ml, Sigma-Aldrich) for 4 h at 5 % CO₂/37 °C. The medium was aspirated from the well without disturbing the MTT

formazan crystals. Then, 200 µl DMSO was added to each well, the plates were shaken for 15 min on a plate shaker at room temperature. Cell viability was determined by measuring the optical density at 570 nm using an ELISA plate reader (BioTek, Burlington, VT, USA). In mouse RPE, cell viability represented the optical density ratio of RPE relative to that of unstimulated WT RPE. In ARPE-19 cells, cell viability represented the optical density ratio of ARPE-19 cells to that of unstimulated control ARPE-19 cells.

Detection of apoptosis by flow cytometry

For evaluation of apoptosis, carefully trypsinized RPE cells were collected and washed twice in PBS with 10 % FBS. The cells were stained with an Annexin V apoptosis detection kit I (BD Biosciences, San Diego, CA, USA), according to the manufacturer's instructions. Fifty thousand events per sample of primary mouse RPE cells and 300,000 events per sample of ARPE-19 cells were acquired with a flow cytometer (FACSCalibur, BD Biosciences, San Jose, CA, USA). All the data were analyzed by FlowJo V.7.6 software (Tree Star, Inc., Ashland, OR, USA).

RNA isolation and quantitative RT-PCR

Total RNA was isolated from RPE cells by an extraction method (TRIzol-phenol-chloroform; Invitrogen, Carlsbad, CA) and treated with DNase I (Qiagen, Hilden, Germany). Equal amounts of RNA were reverse transcribed with Superscript II RNase H Reverse Transcriptase (Invitrogen, Grand Island, NY, USA). Quantitative RT-PCR (qRT-PCR) was performed on the resulting cDNA using Brilliant SYBR Green QPCR Master Mix (Stratagene, La Jolla, CA, USA). The comparative cycle threshold value (Ct) method, representing log transformation, was used to establish relative quantification of the fold changes in gene expression using Stratagene M × 3000P QPCR System (SABiosciences, Frederick, MD, USA). Each 25 µl reaction volume contained 2× PCR master mix (SYBR Green/Rox; SABiosciences), 0.4 µM of each primer, and 2 µl cDNA. The cDNA was amplified with specific primers for 40 cycles. For an internal control, *β-actin* was amplified with a sense primer (5'-TCCCCAACTTGAGATGTATGAAG-3') and an antisense primer (5'-AACTGGTCTCAAGTCAGTGTACAGG-3'). Primers of *FasL*, *Fas*, and *Fas-associated death domain protein (FADD)* were purchased from SABiosciences.

Immunohistochemistry

The RPE cells were seeded at 1×10^5 cells per well in 8-well chamber slides. Cultured cells and retinal tissue for immunohistochemical analyses were fixed, blocked, and incubated overnight with primary antibodies to the

following antigens: FasL (reacts with mouse), 1:100 (Santa Cruz); FasL (reacts with human), 1:100 (Abcam, Inc., Cambridge, MA); Fas, 1:100 (Santa Cruz); cleaved caspase-3, 1:200 (Cell Signaling Technology, Danvers, MA); and cleaved caspase-9, 1:200 (Cell Signaling Technology). After washing, secondary antibodies conjugated to either Alexa-488 or Alexa-555 (1:200, Invitrogen, Eugene, OR, USA) and 4',6-diamidino-2-phenylindole dihydrochloride (DAPI, 1:1000, Invitrogen) were added and incubated for 1 h. The stained retinal tissue or RPE cells were examined under Olympus FV1000 Confocal Scanning Scope.

Statistical analysis

Statistical analyses were performed using SPSS version 17.0 (SPSS, Chicago, IL, USA). Unpaired *t*-tests or analysis of variance (ANOVA) were used to determine whether differences existed between experimental mean values. A *p* value <0.05 was considered statistically significant.

Results

Increased apoptosis in DKO mice retina

Immunohistochemistry was used to detect FasL and Fas expression in the retina of DKO and WT mice under physiological conditions. The data demonstrated stronger immunoreactivity against FasL and Fas in DKO RPE when compared with WT RPE (Fig. 1). Positive expression of FasL and Fas were also noted in DKO retinal lesions, mainly in the inner and outer segments of photoreceptors. These results suggest that DKO RPE is more prone than WT RPE to FasL-mediated apoptosis in physiological conditions.

Enhanced apoptosis in cultured DKO RPE versus WT RPE under inflammatory and oxidative stress

MTT assay showed a similar percentage of cell viability between untreated DKO and WT primary RPE (Fig. 2a). When RPE was stimulated with LPS, TCDD, or H₂O₂, cell viability reduced more in DKO RPE than WT RPE. After primary mouse RPE was stimulated with LPS, TCDD, or H₂O₂, the positive Annexin V and negative PI staining, an index of early apoptotic cells, was higher in DKO RPE than WT RPE with the stimuli by flow cytometry (Fig. 2b). To determine the apoptosis pathway in mouse RPE, *Fasl* and *Fas* mRNA expression was assessed in primary mouse RPE. The results of qRT-PCR showed that *Fasl* and *Fas* transcripts were low and comparable in untreated DKO and WT RPE cells (Fig. 2c, d). When RPE cells were stimulated with LPS, TCDD, or H₂O₂, *Fasl* and *Fas* transcripts increased more in DKO RPE than in WT RPE (Fig. 2c, d).

After evaluation of *Fasl* and *Fas* transcripts in the stimulated mouse RPE, FasL, Fas, cleaved caspase-3, and cleaved caspase-9 proteins were examined subsequently to assess cell apoptosis. Immunohistochemistry showed that expression of FasL and Fas proteins and cleavage of caspase-3 and caspase-9 were higher in DKO RPE than in WT RPE with the stimuli (Fig. 2e–h). Taken together, the data demonstrate that primary RPE cells underwent apoptosis via a FasL-mediated pathway under either inflammatory or oxidative stress. Moreover, DKO RPE is more susceptible to FasL-mediated apoptosis than WT RPE under the stress.

Increased mitochondrial damage of ARPE-19 cells under inflammatory and oxidative stress

ARPE-19 cells were used and cell apoptosis was examined under inflammatory and oxidative stress. MTT data showed decreased cell viability when ARPE-19 cells were stimulated with LPS, TCDD or H₂O₂ (Fig. 3) in a concentration-ranging response respectively (data not shown). The data demonstrate that LPS, TCDD or H₂O₂ stimulation can effectively cause mitochondrial damage in ARPE-19 cells and result in more cell death ultimately.

DcR3 expression and DcR3 knockdown in ARPE-19 cells

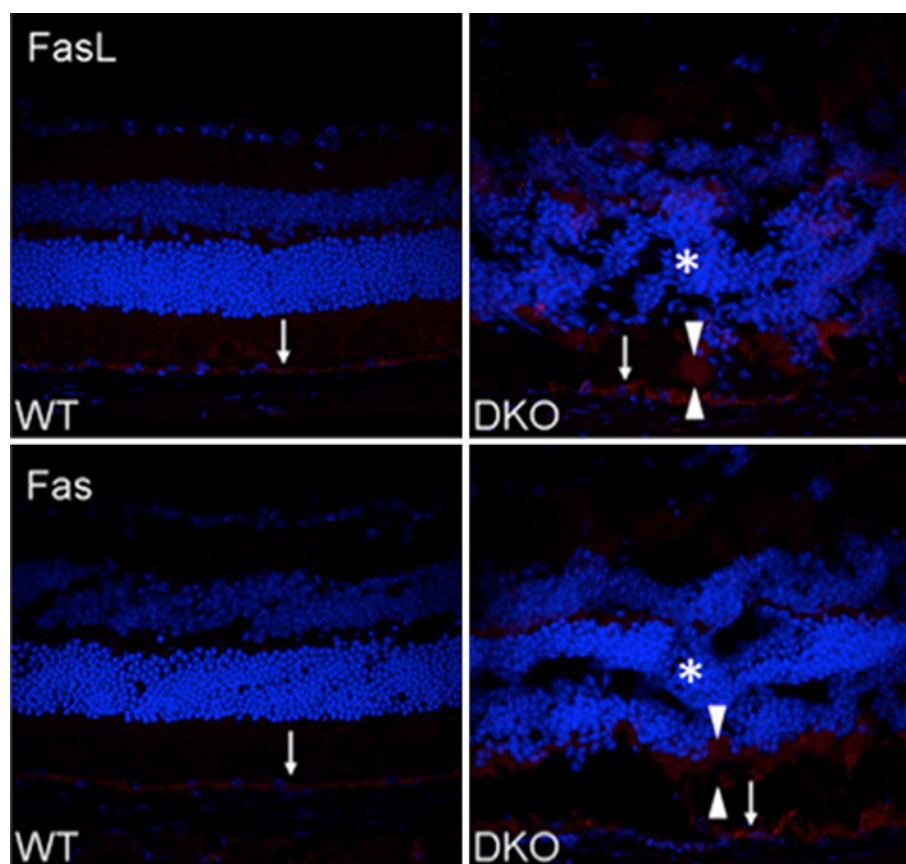
To investigate whether DcR3 is expressed in normal human RPE and ARPE-19 cells, qRT-PCR and immunohistochemistry were performed. Higher *DcR3* mRNA expression was found in control than DcR3 knockdown ARPE-19 cells by qRT-PCR (Fig. 4a). Through immunohistochemistry, endogenous DcR3 protein expression was observed in the cytoplasm of both normal human RPE and ARPE-19 cells (Fig. 4b, c).

When DcR3 expression was confirmed in ARPE-19 cells, DcR3 siRNA was applied to knockdown DcR3 in ARPE-19 cells for different time points. By qRT-PCR analysis, the expression of *DcR3* mRNA in ARPE-19 cells was lower at 12 and 24 h after transfection with DcR3 siRNA and reached a comparable level at 36 h compared with control siRNA (Fig. 4a). Immunohistochemistry confirmed that the expression of DcR3 protein was decreased at 12 and 24 h after transfection with DcR3 siRNA and returned to normal level at 36 h after siRNA transfection (Fig. 4d).

Loss of DcR3 increases ARPE-19 cells apoptosis under inflammatory and oxidative stress

When DcR3 was successfully knocked down in ARPE-19 cells at 12 h after incubation with DcR3 siRNA, DcR3 knockdown ARPE-19 cells were stimulated with LPS, TCDD or H₂O₂. Apoptosis was also assessed by MTT

Fig. 1 Fluorescence micrograph showed increased FasL and Fas expression (red) in DKO RPE than WT RPE (arrows) under physiological conditions. Positive immunoreactivity against FasL and Fas was also detected in the inner and outer segments (between arrowheads) beneath the outer nuclear layer (asterisk) of retinal lesions in DKO. The nuclei were stained with DAPI (blue)



assay, Annexin V and 7-aminoactinomycin D (7-AAD) apoptosis assay, qRT-PCR and immunohistochemistry.

Compared with controls, MTT assay showed less cell viability in DcR3 knockdown ARPE-19 cells under each stimulus (Fig. 5a). Annexin V and 7-AAD apoptosis assay showed a higher percentage of early apoptosis (positive Annexin V and negative 7-AAD staining) in DcR3 knockdown ARPE-19 cells than in controls under each stimulus (Fig. 5b). *FasL* and *Fas* mRNA expression was also increased in DcR3 knockdown ARPE-19 cells under each stimulus (Fig. 5c, d). Higher levels of FasL, Fas, cleaved caspase-3, and cleaved caspase-9 proteins were also observed in DcR3 knockdown cells under the stimuli (Fig. 5e–h). This data indicates that knockdown of DcR3 in ARPE-19 cells causes increased apoptosis under inflammatory and oxidative stress.

Exogenous DcR3 decreases ARPE-19 cells apoptosis under inflammatory and oxidative stress

To investigate whether addition of DcR3 protein can protect against inflammatory and oxidative stress, ARPE-19 cells were preincubated with DcR3 and then stimulated with LPS, TCDD or H₂O₂. MTT assay showed improved cell survival in DcR3 preincubated cells than in controls under each stimulus (Fig. 6a). Apoptosis assay showed a lower percentage of early apoptosis in DcR3 preincubated

cells than in controls under the stimuli (Fig. 6b). *FasL* and *Fas* mRNA expression was also decreased in DcR3 preincubated cells under the stimuli (Fig. 6c, d). Furthermore, a lower expression of FasL, Fas, cleaved caspase-3, and cleaved caspase-9 was observed in DcR3 preincubated cells under the stimuli (Fig. 6e–h). These results demonstrate that DcR3 protects ARPE-19 cells from apoptosis under inflammatory and oxidative stress.

Discussion

Up until now, no extensive studies on apoptosis in DKO/*Crb1*^{rd8} mice and their RPE cells have been reported; although photoreceptor cell death is well documented in human inherited retinal degeneration such as retinitis pigmentosa and mice with retinal degeneration such as rd1 mouse [29–31]. Previously, we reported no significant difference in expression of *Fas* and *Fasl* transcripts between DKO and WT eyes [32]. In this study, we found higher expression of Fas and FasL proteins in DKO retina than that in WT retina. Although it is not common, the discordant mRNA and protein in the same tissue has been documented in other studies [33–35]. Based on our results, FasL and Fas protein translation rather than transcription in the DKO retina could be more indicative of biologic

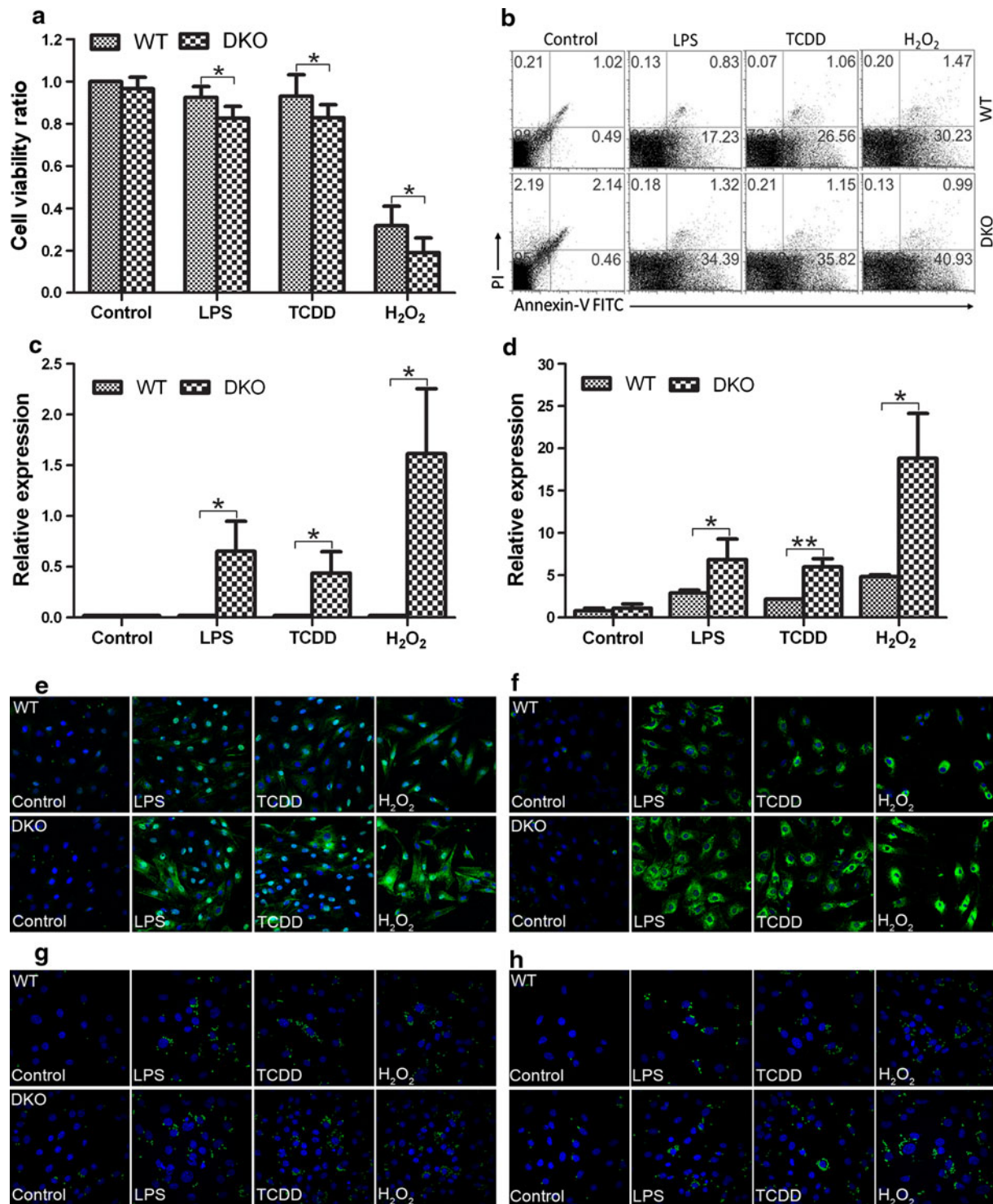


Fig. 2 RPE apoptosis is higher in DKO mice than WT mice under 1 μg/ml LPS, 1 nM TCDD, or 100 μM H₂O₂ stimulation. **a** MTT assay showed less cell viability in DKO RPE than WT RPE under each stimulation ($n = 7$). Each cell viability trial was evaluated against the control WT RPE cells (designated as baseline 1); **b** Annexin V and propidium iodide (PI) apoptosis assay showed a higher percentage of apoptosis in DKO RPE than WT RPE with stimulation ($n = 3$); **c**, **d** qRT-PCR showed increased *FasL* and *Fas*

mRNA expression in DKO RPE than WT RPE under each stimulus ($n = 3$); **e–h** immunofluorescence micrograph showed higher FasL (**e**, green), Fas (**f**, green), cleaved caspase-3 (**g**, green), and cleaved caspase-9 (**h**, green) expression in DKO RPE than WT RPE with stimulation ($n = 3$). The nuclei were stained with DAPI (blue). The data are represented as mean ± SD. * $p < 0.05$; ** $p < 0.01$ compared between WT and DKO

functionality and importance. We also demonstrated that DKO RPE is more prone to FasL-mediated apoptosis than WT RPE under either inflammatory stimulation or oxidative stress. Moreover, FasL-mediated apoptosis in human ARPE-19 cells under similar stimuli is confirmed by adding or knocking down DcR3.

Geographic atrophy AMD is characterized by presence of drusen, photoreceptor degeneration, thickening of Bruch's membrane, and hypopigmentation, attenuation or atrophy of RPE in the macular area. The DKO mice in our study have deficiency of *Ccl2* and *Cx3Cr1* on *Crb1^{rd8}* background [27]. Fundoscopy of the DKO mouse shows multiple deep retinal lesions emerging at approximately 4 weeks of age, which worsen and become confluent with aging [27]. Histology also demonstrates focal photoreceptor disorganization, degeneration

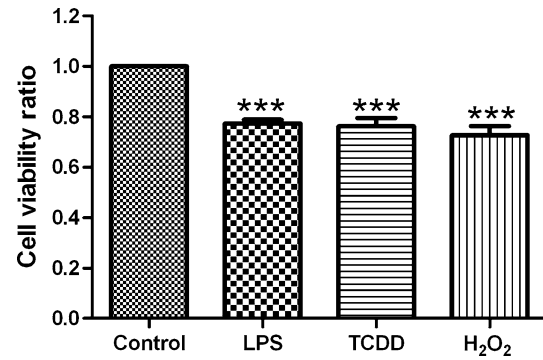


Fig. 3 Decreased cell viability in ARPE-19 cells when treated with 10 μ g/ml LPS, 10 nM TCDD, or 200 μ M H₂O₂. The data are represented as mean \pm SD ($n = 3$). *** $p < 0.001$ compared with control

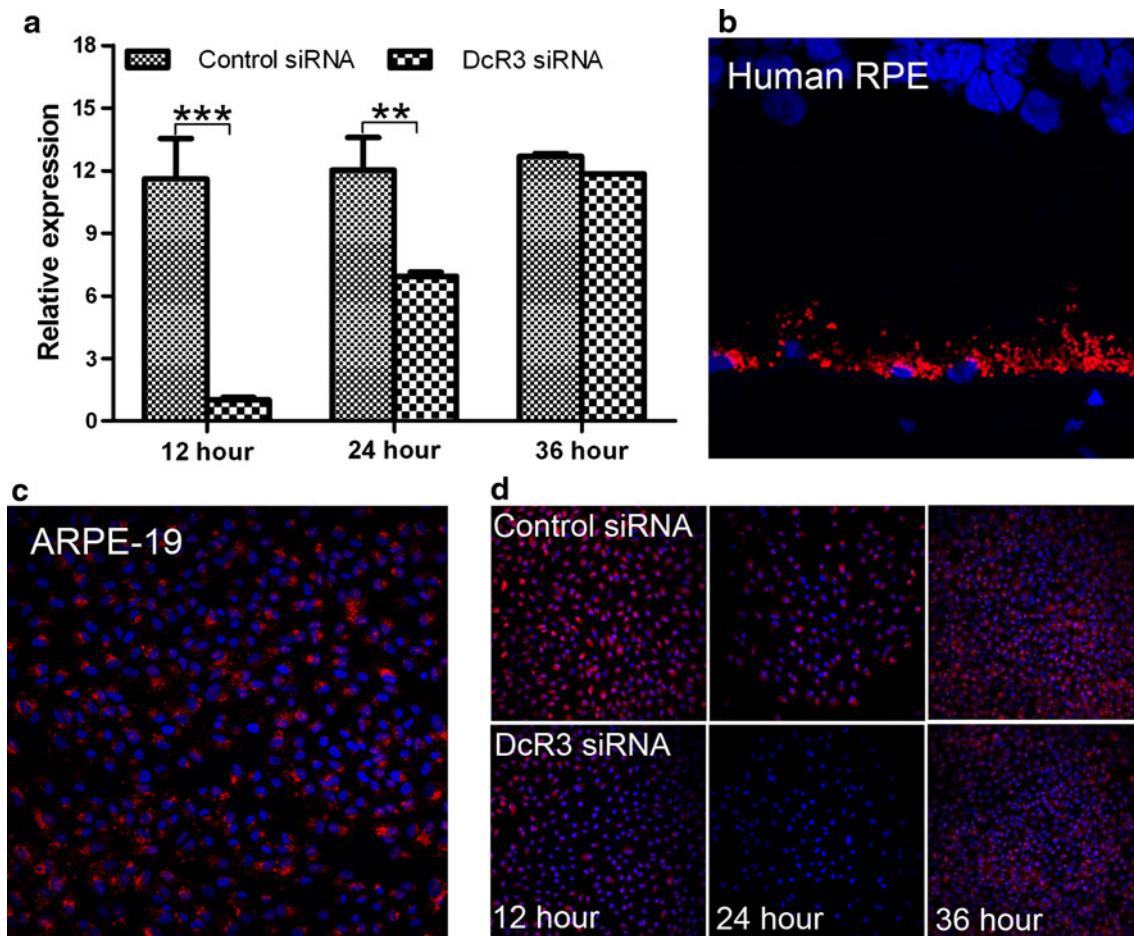


Fig. 4 DcR3 is expressed in APRE-19 cells and DcR3 siRNA induces reduction of DcR3 expression. **a** *DcR3* mRNA was consistently expressed in control siRNA transfected ARPE-19 cells at 12, 24, and 36 h after transfection. In comparison, *DcR3* mRNA expression in DcR3 siRNA transfected ARPE-19 cells was maximally decreased at 12 h, remained decreased at 24 h, and reached comparable expression with controls at 36 h; **b** immunofluorescence show DcR3 (red) was expressed in the cytoplasm of normal human RPE

cells; **c** immunofluorescence show DcR3 (red) was expressed in the cytoplasm of ARPE-19 cells; **d** immunofluorescence show DcR3 (red) expression in DcR3 siRNA transfected ARPE-19 cells was decreased at 12 h, reached maximal decrease at 24 h, and returned to normal levels at 36 h. The nuclei were stained with DAPI (blue). The data are represented as mean \pm SD ($n = 3$). ** $p < 0.01$; *** $p < 0.001$ compared between control siRNA and DcR3 siRNA

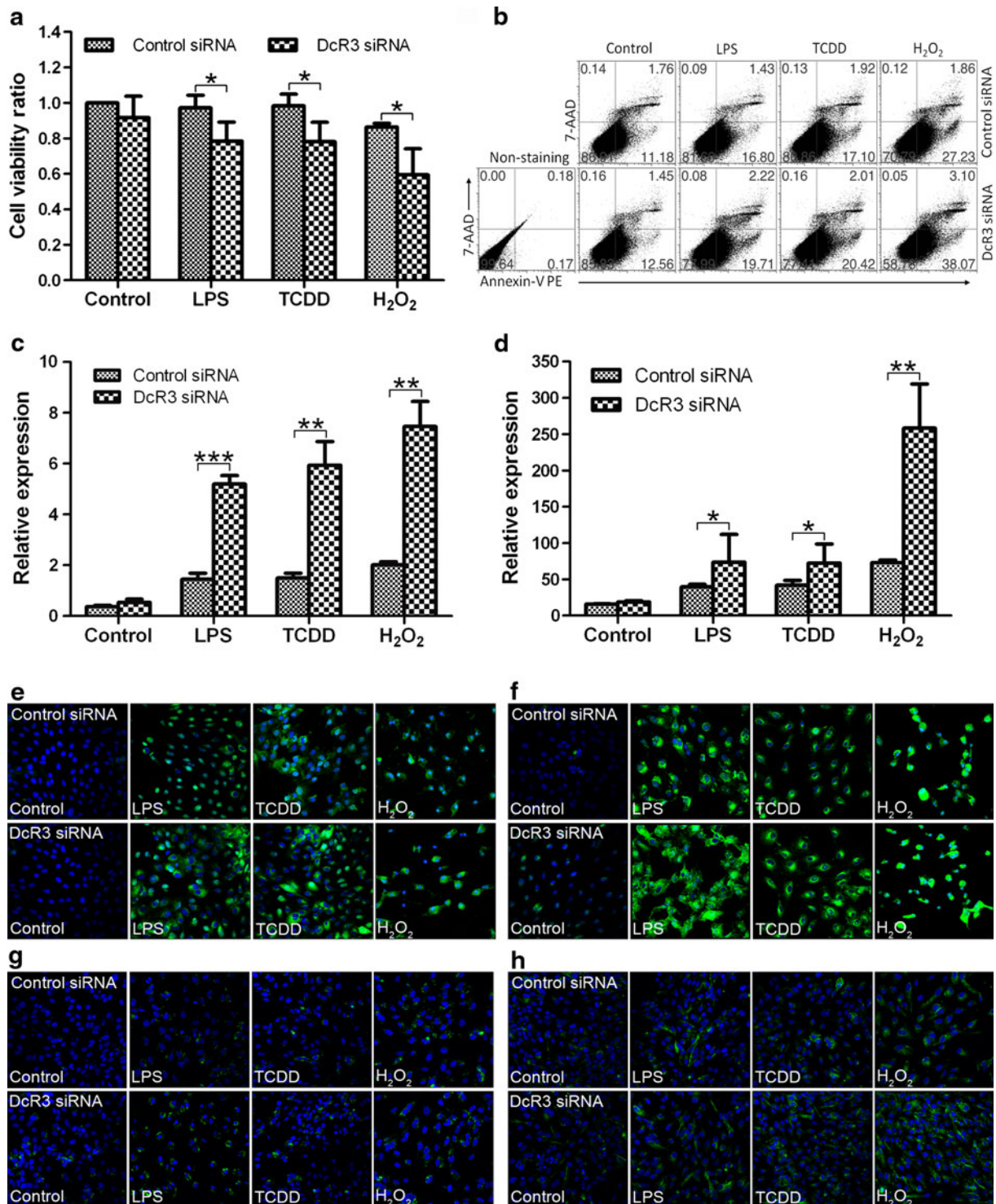


Fig. 5 Knockdown of DcR3 induces apoptosis in ARPE-19 cells under LPS, TCDD, or H₂O₂ stimulation. **a** MTT assay showed less cell viability in DcR3 knockdown ARPE-19 cells than in controls under each stimulus. Each cell viability trial was evaluated against the unstimulated cells transfected with control siRNA (designated as baseline 1); **b** Annexin V and 7-AAD apoptosis assay showed a higher percentage of apoptosis in DcR3 knockdown ARPE-19 cells than in controls under the stimuli; **c**, **d** *FasL* (**c**) and *Fas* (**d**) mRNA expression was increased in DcR3 knockdown ARPE-19 cells under each stimulus; **e–h**

immunofluorescence micrograph showed higher expression of FasL (**e**, green), Fas (**f**, green), cleaved caspase-3 (**g**, green), and cleaved caspase-9 (**h**, green) in DcR3 knockdown ARPE-19 cells than in controls with LPS and TCDD stimulation. Enhanced expression of FasL, Fas, cleaved caspase-3, and cleaved caspase-9 was comparable between control and DcR3 knockdown ARPE-19 cells under H₂O₂ stimulation. The nuclei were stained with DAPI (blue). The data are represented as mean ± SD (*n* = 3). **p* < 0.05; ***p* < 0.01; ****p* < 0.001 compared between control siRNA and DcR3 siRNA

and atrophy, focal RPE hypopigmentation and vacuolation, and thickening of Bruch's membrane, corresponding to some deep retinal lesions under funduscopy [27]. Some other fundoscopic lesions may represent retinal dystrophy from *Crb1^{rd8}* background. High retinal A2E, a biochemical marker for AMD, is also detected in these mice [27]. Because of similar immunopathological and biochemical features between human AMD and the DKO mouse model, the latter has been used as a suitable model for AMD studies.

By having photoreceptor and RPE abnormalities, strong immunoreactivity against FasL and Fas protein were noted in both photoreceptor and RPE lesion area of DKO mouse spontaneously. This findings correlate well with the report that strong Fas signals are expressed in the photoreceptors of human AMD eyes; in contrast, Fas protein is nearly undetectable in normal human photoreceptors [14]. Because FasL/Fas interaction is one of the main pathways involved in cell apoptosis, it is logical to investigate whether RPE would undergo enhanced apoptosis via FasL-mediated pathway in the DKO AMD mouse model.

Inflammation and oxidative stress are considered to be highly involved in the pathogenesis of AMD. Additionally, RPE is regarded as a pivotal cell in AMD initiation and progression. Thus, stimulation mimicking inflammatory and oxidative stress was used to challenge RPE cells and verify the FasL-mediated pathway in RPE apoptosis. LPS and H₂O₂ have been successfully used to induce inflammatory and oxidative stress, respectively, in RPE cells [36, 37]. Meanwhile, TCDD, a member of the polychlorinated dibenzo-*p*-dioxin family, was first used in RPE cells to induce oxidative stress. During subacute and chronic exposure, TCDD induces DNA damage and oxidative stress in mammalian cells via activation of aryl hydrocarbon receptor and expression of cytochrome P450 [38–40]. DKO RPE showed enhanced RPE apoptosis via FasL-mediated pathway under either inflammatory or oxidative stress.

Given that inflammatory and oxidative stress are capable of enhancing FasL-mediated apoptosis in DKO RPE, human ARPE-19 cells were also stimulated with LPS, TCDD, or H₂O₂ to further investigate the FasL/Fas pathway on apoptosis. The ARPE-19 cell line has been established by selective trypsinization of a primary human RPE culture and is frequently used for studies of RPE physiology [41]. In this study, we found higher levels of *Fas* and *FasL* mRNA but no difference in *FADD* mRNA (data not shown) after the cells were stimulated with H₂O₂. Previously we also reported no difference in *FADD* transcripts in ARPE-19 cells treated with H₂O₂ [32]. *FADD* is an adaptor molecule in the Fas-mediated apoptosis pathway. There are other adaptors, such as tumor necrosis factor receptor-associated death domain protein (TRADD), which may mediate cell death as well. In addition, apoptosis is controlled by multiple intracellular and extracellular signals with complicated interactions. Studies have

demonstrated inconsistent levels between Fas and FADD in the same cell [42, 43].

FasL-mediated apoptosis in ARPE-19 cells was further investigated by adding or knocking down DcR3, which is capable of neutralizing the biological effects of three TNF superfamily (TNFSF) members: FasL, LIGHT, and TNF-like molecule 1A (TL1A). As a soluble decoy receptor, DcR3 competitively binds with FasL but does not transduce apoptotic signals [24, 25]. DcR3 is strongly expressed in normal human RPE and ARPE-19 cells, indicating DcR3 might act as a factor to protect RPE from apoptosis in physiological conditions. By knocking down DcR3 expression during a certain period of time, the stressed ARPE-19 cells showed enhanced apoptosis and greatly increased expression of cleaved caspase-3 and cleaved caspase-9 after LPS and TCDD stimulation which indicated increased cellular apoptosis.

Increased *FasL* and *Fas* transcripts as well as FasL and Fas proteins were also found in DcR3 knockdown ARPE-19 cells under the stress. This could result from modulation of Fas and FasL expression in different mechanism. FasL is reported to participate in a positive feedback loop of apoptosis [44]. The activation of caspases can act as significant modulators of FasL expression. Moreover, induction of Bim, a member of the pro-apoptotic Bcl-2 family, is reported to induce FasL expression through a caspase-dependent mechanism [45]. Thus, enhanced apoptosis with increased density of caspases and pro-apoptotic factors may further upregulate FasL expression. Indeed, DNA damage can cause apoptosis and also upregulate Fas expression. Our data show the positive feedback loop with a trend of increased Fas expression in the apoptotic ARPE-19 cells. On the contrary, pre-incubation with exogenous DcR3 in stressed ARPE-19 showed less cell apoptosis and reduced FasL and Fas expression in both mRNA and protein levels.

However, our results also showed that the increased FasL, Fas, and cleavage of caspase-3 and caspase-9 are similar between both experimental groups, control siRNA versus DcR3 siRNA transfected ARPE-19 cells, and control versus DcR3 pre-incubated ARPE-19 cells under H₂O₂ stimulation, despite the fact that *FasL* and *Fas* mRNA were significantly different between each group. The variances may be explained by the differing mechanisms of oxidative stress between TCDD and H₂O₂ as well as the concentration dependent nature of these stimulants [37–40]. Thus, the change in mRNA expression of *Fas* and *FasL* in H₂O₂ stimulated ARPE-19 cells may not necessarily correlate with marked elevation of FasL, Fas, cleaved caspase-3, and cleaved caspase-9. Furthermore, the intrinsic pathway could play an important role in the varied expression levels of caspase-3 and caspase-9 upon inflammatory and oxidative stress [23].

In summary, our study demonstrates that the FasL-mediated pathway contributes towards the enhanced

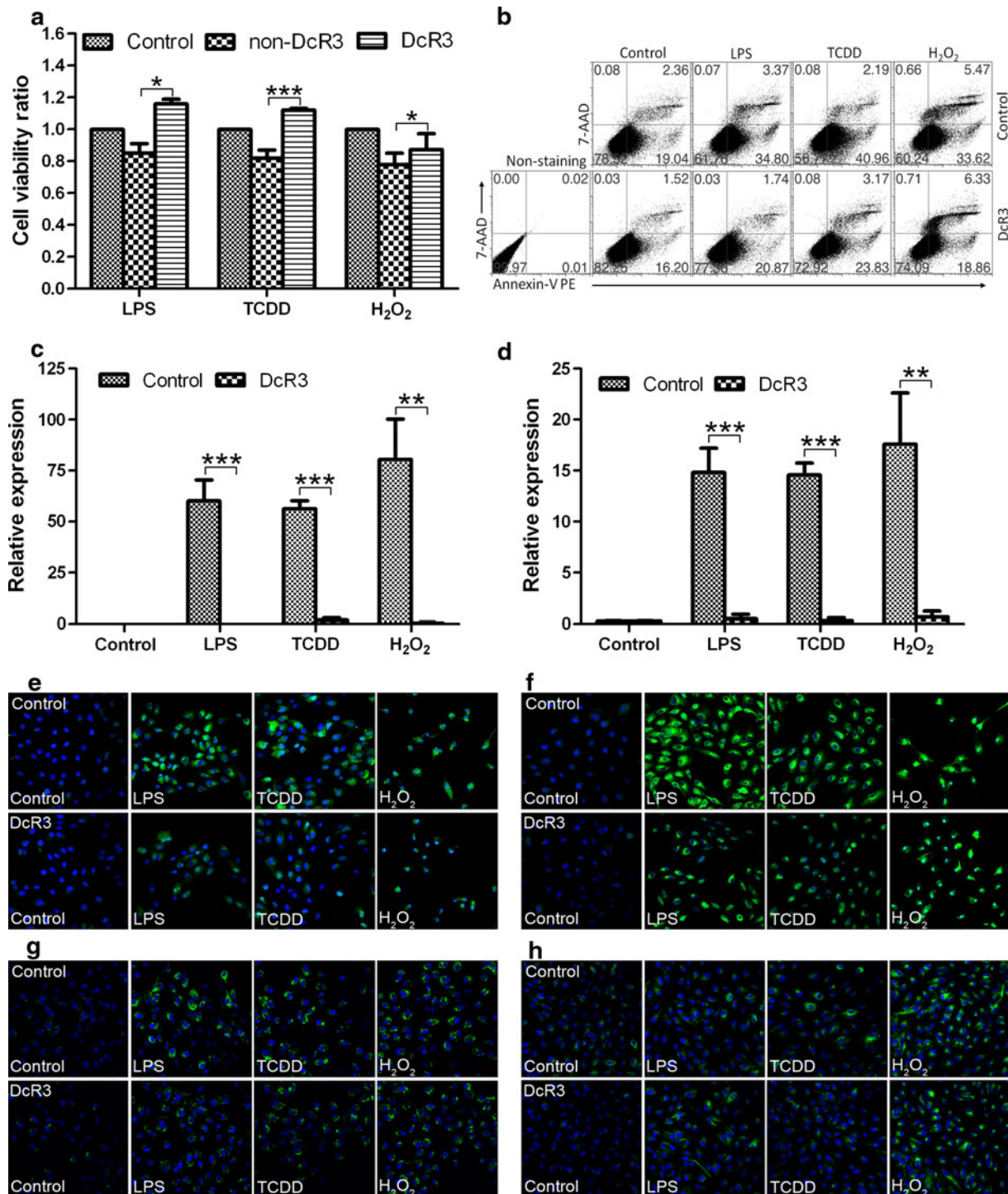


Fig. 6 Addition of DcR3 decreases ARPE-19 apoptosis under LPS, TCDD, or H₂O₂ stimulation. **a** MTT assay showed more cell viability in DcR3 pre-incubated ARPE-19 cells than in controls under each stimulus. Each cell viability trial was evaluated against the control unstimulated cells (designated as baseline 1); **b** Annexin V and 7-AAD apoptosis assay showed a lower percentage of apoptosis in DcR3 preincubated ARPE-19 cells than in controls under the stimuli; **c**, **d** *FasL* (**c**) and *Fas* (**d**) mRNA expression was decreased in DcR3 preincubated ARPE-19 cells under each stimulus;

e–h immunofluorescence micrograph showed lower expression of FasL (**e**, green), Fas (**f**, green), cleaved caspase-3 (**g**, green), and cleaved caspase-9 (**h**, green) in DcR3 preincubated ARPE-19 cells than in controls with LPS and TCDD stimulation. Enhanced expression of FasL, Fas, cleaved caspase-3, and cleaved caspase-9 was comparable between control and DcR3 preincubated ARPE-19 cells under H₂O₂ stimulation. The nuclei were stained with DAPI (blue). The data are represented as mean \pm SD ($n = 3$). * $p < 0.05$; ** $p < 0.01$; *** $p < 0.001$ compared between control and DcR3

apoptosis under both inflammatory and oxidative stress in ARPE-19 cells and the DKO RPE. RPE apoptosis is regarded as a pivotal factor and contributes to AMD pathogenesis.

Acknowledgments The National Eye Institute Intramural Research Program supported the study.

Conflict of interest None.

References

- World Health Organization (2011) Visual impairment and blindness. <http://www.who.int/mediacentre/factsheets/fs282/en/index.html>. Accessed 6 November 2011
- Friedman DS, O'Colmain BJ, Munoz B, Tomany SC, McCarty C, de Jong PT, Nemesure B, Mitchell P, Kempen J (2004) Prevalence of age-related macular degeneration in the United States. *Arch Ophthalmol* 122:564–572
- Coleman HR, Chan CC, Ferris FL 3rd, Chew EY (2008) Age-related macular degeneration. *Lancet* 372:1835–1845
- Klein R, Peto T, Bird A, Vannewkirk MR (2004) The epidemiology of age-related macular degeneration. *Am J Ophthalmol* 137:486–495
- Ferris FL 3rd, Fine SL, Hyman L (1984) Age-related macular degeneration and blindness due to neovascular maculopathy. *Arch Ophthalmol* 102:1640–1642
- Boulton M, Dayhaw-Barker P (2001) The role of the retinal pigment epithelium: topographical variation and ageing changes. *Eye* 15:384–389
- Feher J, Kovacs I, Artico M, Cavallotti C, Papale A, Balacco Gabrieli C (2006) Mitochondrial alterations of retinal pigment epithelium in age-related macular degeneration. *Neurobiol Aging* 27:983–993
- Detrick B, Hooks JJ (2010) Immune regulation in the retina. *Immunol Res* 47:153–161
- Chin MS, Nagineni CN, Hooper LC, Detrick B, Hooks JJ (2001) Cyclooxygenase-2 gene expression and regulation in human retinal pigment epithelial cells. *Invest Ophthalmol Vis Sci* 42:2338–2346
- Momma Y, Nagineni CN, Chin MS, Srinivasan K, Detrick B, Hooks JJ (2003) Differential expression of chemokines by human retinal pigment epithelial cells infected with cytomegalovirus. *Invest Ophthalmol Vis Sci* 44:2026–2033
- Liang FQ, Godley BF (2003) Oxidative stress-induced mitochondrial DNA damage in human retinal pigment epithelial cells: a possible mechanism for RPE aging and age-related macular degeneration. *Exp Eye Res* 76:397–403
- Augustin AJ, Kirchhof J (2009) Inflammation and the pathogenesis of age-related macular degeneration. *Expert Opin Ther Targets* 13:641–651
- Jiang S, Moriarty-Craige SE, Li C, Lynn MJ, Cai J, Jones DP, Sternberg P (2008) Associations of plasma-soluble fas ligand with aging and age-related macular degeneration. *Invest Ophthalmol Vis Sci* 49:1345–1349
- Dunaief JL, Dentchev T, Ying GS, Milam AH (2002) The role of apoptosis in age-related macular degeneration. *Arch Ophthalmol* 120:1435–1442
- Anderson DH, Mullins RF, Hageman GS, Johnson LV (2002) A role for local inflammation in the formation of drusen in the aging eye. *Am J Ophthalmol* 134:411–431
- Bazan NG, Calandria JM, Serhan CN (2010) Rescue and repair during photoreceptor cell renewal mediated by docosahexaenoic acid-derived neuroprotectin D1. *J Lipid Res* 51:2018–2031
- Nilsson SE, Sundelin SP, Wihlmark U, Brunk UT (2003) Aging of cultured retinal pigment epithelial cells: oxidative reactions, lipofuscin formation and blue light damage. *Doc Ophthalmol* 106:13–16
- Liles MR, Newsome DA, Oliver PD (1991) Antioxidant enzymes in the aging human retinal pigment epithelium. *Arch Ophthalmol* 109:1285–1288
- Cai J, Nelson KC, Wu M, Sternberg P Jr, Jones DP (2000) Oxidative damage and protection of the RPE. *Prog Retin Eye Res* 19:205–221
- Fujihara M, Nagai N, Sussan TE, Biswal S, Handa JT (2008) Chronic cigarette smoke causes oxidative damage and apoptosis to retinal pigmented epithelial cells in mice. *PLoS ONE* 3:e3119
- Ding X, Patel M, Shen D, Herzlich AA, Cao X, Villasmil R, Klupsch K, Tuo J, Downward J, Chan CC (2009) Enhanced HtrA2/Omi expression in oxidative injury to retinal pigment epithelial cells and murine models of neurodegeneration. *Invest Ophthalmol Vis Sci* 50:4957–4966
- Bertram KM, Baglolle CJ, Phipps RP, Libby RT (2009) Molecular regulation of cigarette smoke induced-oxidative stress in human retinal pigment epithelial cells: implications for age-related macular degeneration. *Am J Physiol Cell Physiol* 297:C1200–C1210
- Igney FH, Krammer PH (2002) Death and anti-death: tumour resistance to apoptosis. *Nat Rev Cancer* 2:277–288
- Pitti RM, Marsters SA, Lawrence DA, Roy M, Kischkel FC, Dowd P, Huang A, Donahue CJ, Sherwood SW, Baldwin DT, Godowski PJ, Wood WI, Gurney AL, Hillan KJ, Cohen RL, Goddard AD, Botstein D, Ashkenazi A (1998) Genomic amplification of a decoy receptor for Fas ligand in lung and colon cancer. *Nature* 396:699–703
- Lin WW, Hsieh SL (2011) Decoy receptor 3: a pleiotropic immunomodulator and biomarker for inflammatory diseases, autoimmune diseases and cancer. *Biochem Pharmacol* 81:838–847
- Bai C, Connolly B, Metzker ML, Hilliard CA, Liu X, Sandig V, Soderman A, Galloway SM, Liu Q, Austin CP, Caskey CT (2000) Overexpression of M68/DcR3 in human gastrointestinal tract tumors independent of gene amplification and its location in a four-gene cluster. *Proc Natl Acad Sci U S A* 97:1230–1235
- Tuo J, Bojanowski CM, Zhou M, Shen D, Ross RJ, Rosenberg KI, Cameron DJ, Yin C, Kowalak JA, Zhuang Z, Zhang K, Chan CC (2007) Murine ccl2/cx3cr1 deficiency results in retinal lesions mimicking human age-related macular degeneration. *Invest Ophthalmol Vis Sci* 48:3827–3836
- Chan CC, Ross RJ, Shen D, Ding X, Majumdar Z, Bojanowski CM, Zhou M, Salem N Jr, Bonner R, Tuo J (2008) Ccl2/Cx3cr1-deficient mice: an animal model for age-related macular degeneration. *Ophthalmic Res* 40:124–128
- Sancho-Pelluz J, Arango-Gonzalez B, Kustermann S, Romero FJ, van Veen T, Zrenner E, Ekstrom P, Paquet-Durand F (2008) Photoreceptor cell death mechanisms in inherited retinal degeneration. *Mol Neurobiol* 38:253–269
- Portera-Cailliau C, Sung CH, Nathans J, Adler R (1994) Apoptotic photoreceptor cell death in mouse models of retinitis pigmentosa. *Proc Natl Acad Sci U S A* 91:974–978
- Sanges D, Comitato A, Tammara R, Marigo V (2006) Apoptosis in retinal degeneration involves cross-talk between apoptosis-inducing factor (AIF) and caspase-12 and is blocked by calpain inhibitors. *Proc Natl Acad Sci U S A* 103:17366–17371
- Cao X, Liu M, Tuo J, Shen D, Chan CC (2010) The effects of quercetin in cultured human RPE cells under oxidative stress and in Ccl2/Cx3cr1 double deficient mice. *Exp Eye Res* 91:15–25

33. Maier T, Guell M, Serrano L (2009) Correlation of mRNA and protein in complex biological samples. *FEBS Lett* 583:3966–3973
34. Greenbaum D, Colangelo C, Williams K, Gerstein M (2003) Comparing protein abundance and mRNA expression levels on a genomic scale. *Genome Biol* 4:117
35. Schwanhausser B, Busse D, Li N, Dittmar G, Schuchhardt J, Wolf J, Chen W, Selbach M (2011) Global quantification of mammalian gene expression control. *Nature* 473:337–342
36. Cho Y, Cao X, Shen D, Tuo J, Parver LM, Rickles FR, Chan CC (2011) Evidence for enhanced tissue factor expression in age-related macular degeneration. *Lab Invest* 91:519–526
37. Kaczara P, Sarna T, Burke JM (2010) Dynamics of H₂O₂ availability to ARPE-19 cultures in models of oxidative stress. *Free Radic Biol Med* 48:1064–1070
38. Lin PH, Lin CH, Huang CC, Chuang MC, Lin P (2007) 2,3,7,8-Tetrachlorodibenzo-*p*-dioxin (TCDD) induces oxidative stress, DNA strand breaks, and poly(ADP-ribose) polymerase-1 activation in human breast carcinoma cell lines. *Toxicol Lett* 172:146–158
39. Ilavarasi K, Kiruthiga PV, Pandian SK, Devi KP (2011) Hydroxytyrosol, the phenolic compound of olive oil protects human PBMC against oxidative stress and DNA damage mediated by 2,3,7,8-TCDD. *Chemosphere* 84:888–893
40. Reichard JF, Dalton TP, Shertzer HG, Puga A (2005) Induction of oxidative stress responses by dioxin and other ligands of the aryl hydrocarbon receptor. *Dose Response* 3:306–331
41. Dunn KC, Aotaki-Keen AE, Putkey FR, Hjelmeland LM (1996) ARPE-19, a human retinal pigment epithelial cell line with differentiated properties. *Exp Eye Res* 62:155–169
42. Ahn EY, Pan G, Vickers SM, McDonald JM (2002) IFN-gamma upregulates apoptosis-related molecules and enhances Fas-mediated apoptosis in human cholangiocarcinoma. *Int J Cancer* 100:445–451
43. Aggarwal S, Gupta S (1999) Increased activity of caspase 3 and caspase 8 in anti-Fas-induced apoptosis in lymphocytes from ageing humans. *Clin Exp Immunol* 117:285–290
44. Suhara T, Kim HS, Kirshenbaum LA, Walsh K (2002) Suppression of Akt signaling induces Fas ligand expression: involvement of caspase and Jun kinase activation in Akt-mediated Fas ligand regulation. *Mol Cell Biol* 22:680–691
45. Dijkers PF, Medema RH, Lammers JW, Koenderman L, Coffey PJ (2000) Expression of the pro-apoptotic Bcl-2 family member Bim is regulated by the forkhead transcription factor FKHR-L1. *Curr Biol* 10:1201–1204